Spectroscopic and calorimetric investigation on the DNA triplex formed by d(CTCTTCTTTCTTTTCTTTCTTCTC) and d(GAGAAGAAAGA) at acidic pH

Luigi E.Xodo, Giorgio Manzini and Franco Quadrifoglio[1]
Department of Biochemistry, Biophysics and Macromolecular Chemistry, University of Trieste, 34127 Trieste and [1]Institute of Biology, Faculty of Medicine, University of Udine, 33100 Udine, Italy

Received March 9, 1990; Revised and Accepted May 18, 1990

ABSTRACT

The equimolar mixture of d(CTCTTCTTTCTTTTCTTTCTTCTC) (dY_{24}) and d(GAGAAGAAAGA) (dR_{11}) [designated (dY_{24}).(dR_{11})], forms at pH = 5 a DNA triplex, which mimicks the H-DNA structure. The DNA triplex was identified by the following criteria: (i) dY_{24} and dR_{11} co-migrate in a poly-acrylamide gel, with a mobility and a retardation coefficient comparable to those observed for an 11-triad DNA triplex, previously characterized in our laboratories (1); (ii) the intercalator ethidium bromide shows a poor affinity for (dR_{11}).(dY_{24}) at pH = 5, and a high affinity at pH = 8; (iii) the (dR_{11}).(dY_{24}) mixture is not a substrate for DNase I at pH = 5; (iv) the CD spectrum of (dR_{11}).(dY_{24}), at pH = 5, is consistent with those previously reported for triple-stranded DNA.

The (dR_{11}).(dY_{24}) mixture exhibits a thermally induced co-operative transition, which appears to be monophasic, reversible and concentration dependent. This transition is attributed to the disruption of the DNA triplex into single strands. The enthalpy change of the triplex-coil transition was measured by DSC (ΔHcal = 129 ± 6 kcal/mol) and, assuming a two-state model, by analysis of UV-denaturation curves (average of two methods ΔH_{UV} = 137 ± 13 kcal/mol). Subtracting from ΔHcal of triplex formation the contributions due to the Watson-Crick helix and to the protonation of the C-residues, we found that each pyrimidine binding into the major groove of the duplex, through a Hoogsteen base pair, is accompanied by an average $\Delta H = -5.8 \pm 0.6$ kcal/mol. The effect on the stability of the (dR_{11}).(dY_{24}) triplex due to the substitution of a T:A:T triad with a T:T:T one was also investigated.

INTRODUCTION

Triple-stranded structures (triplexes) formed by DNA and RNA homopolymers were first reported in the sixties (2–4). These studies, together with more recent ones (5–8), have identified the sequence requirements and the pH conditions for the formation of DNA and RNA triplexes. Recently, there is a great deal of interest in the DNA triplexes formed by oligopurine-oligopyrimidine sequences, (dR_n).(dY_n), under the influence of torsional stress and/or low pH (9–13). The (dR_n).(dY_n) sequences are found in the eukaryotic genome with a frequency higher than normal (14,15) and close to regulatory regions (16); for this reason the (dR_n).(dY_n) could have a potential role in the regulation of gene expression (11). The triple-stranded DNA structure formed by (dR_n).(dY_n) sequences has been called H-DNA by Frank-Kamenetskii and co-workers (9,10). In this unusual structure half of the d(Y_n) strand forms a normal Watson-Crick (W.C.) duplex with the (dR_n) strand, while the other half of (dY_n) folds back and binds into the major groove of the W.C. duplex through the formation of Hoogsteen base pairs. In such a structure half of the (dR_n) strand remains unpaired and this feature should explain the hypersensitivity of the (dR_n).(dY_n) sequences for single-stranded specific nucleases (16–18). Two isomers of the H-DNA structure can be formed depending on whether the 3'- or the 5'-half of the (dY_n) strand is involved in intra-molecular base pairing, through a Hoogsteen geometry (10). Another essential requirement for the formation of triple-stranded DNA is that the (dR_n).(dY_n) sequences must have a mirror symmetry, in order to satisfy the specificity of bases in forming the C:G:C^+ and T:A:T triads. In the H-DNA triplex the orientation of the two pyrimidine strands is antiparallel, as found by X-ray diffraction study on fibers of polyA:2polyU and polydA:2polydT (19).

The formation of stable DNA triplexes by short oligodeoxynucleotides has been previously reported (12,20). Thus, the physico-chemical characterization of this unusual DNA structure can be performed using simple molecular models. Two NMR investigations on short DNA triplexes have been reported (21,22).

Recently, we have characterized, by electrophoresis and UV-spectroscopy, the DNA triplex formed by mixing the hairpin form of d(GAAGGAGGAGATTTTTCTCCTCCTTC) with d(CTTCCTCCTCT) (1).

The structure of H-DNA is peculiar in that the (dY_n) strand forms a loop which bridges a triple-stranded stem, i.e the phosphate-phosphate distance between the two pyrimidines of the closing base triads (Scheme 2). We have obtained a DNA triplex with a structure similar to that of H-DNA by mixing oligomers d(CTCTTCTTTCTTTTCTTTCTTCTC) and d(GAGAAGAAAGA) in equimolar ratio. In this communication we report the results of a combined spectroscopic, electrophoretic and calorimetric study on the thermodynamic stability of this DNA

triplex. The effect on the stability of the DNA triplex due to the introduction of a T:T:T mismatched triad was also investigated.

MATERIALS AND METHODS

Samples

The oligodeoxynucleotides d(CTCTTCTTTCTTTTCTTTC-TTCTC) (dY_{24}) d(GAGAAGAAAGA) (dR_{11}) and d(GAGTAGAAAGA) as well as others, of length varying from 12 to 20 base pairs, used as reference in electrophoretic experiments, have been synthesized in solid phase (CPG column), with a standard method based on the phosphoamidite chemistry, implemented on a automatic DNA synthesizer (Applied Biosystems 380B). After base deprotection, the purification was carried out with a G-50 Sephadex resin, by eluting the column with a 0.05 M ammonium bicarbonate. Purity was confirmed by both HPLC and denaturing eletrophoresis (23).

Buffer

The buffers used in this study were: i) 0.1 M sodium acetate (pH=5), 50 mM NaCl, 10 mM $MgCl_2$; ii) 0.1 M Tris.HCl (pH=8), 5 mM $MgCl_2$, 5 mM NaCl. For CD experiments a more diluted buffer at pH=5 was used, as indicated in the figure caption.

Polyacrylamide Electrophoresis

Polyacrylamide gel electrophoresis (PAGE) was carried out on gels (20 or 10×15×0.15 cm) obtained from buffer solutions containing 20% (15% or 25%) (w/v) acrylamide (3.3% bis-acrylamide), 0.07% ammonium persulfate. The stacking gel contained 5% acrylamide. In general the electrophoreses were performed at a constant voltage of 10 V/cm with a current of 20−30 mA. The amount of sample loaded in the gel was in the order of 2−4 μg. Bromphenol blue dye was used as a marker. The bands were stained with 'stains all' dye in 1:1 water-formamide and the gels were photographed after 1 hour.

Circular Dichroism and Fluorescence

Circular dichroism (CD) spectra were obtained with a Jasco J-500 A dichrograph, equipped with a thermostattable cuvette holder which allows measurements at controlled temperature. The dichrograph was connected to a Jasco DP 500 N data processor. Spectra are presented as $\Delta\epsilon = (\epsilon_L - \epsilon_R)$ in units of $M^{-1}cm^{-1}$. The spectra were obtained from sample solutions at a nucleotide concentration in the order of 4 mM. Absorbance of the solvent in the short wavelength region of the spectrum (200−230 nm) was minimized by using a 1 mm pathlength cuvette and as buffer a 1mM sodium acetate (pH=5), 100 mM $NaClO_4$.

Fluorescence measurements were performed with a Perkin-Elmer MPF-3L Spectrofluorometer, in the ratio mode. The excitation and emission wavelengths were 525 and 598 nm, respectively.

Denaturation Experiments

Denaturation experiments were performed on a Cary 219 spectrophotometer (Varian). The temperature was increased at a rate of 0.3°C/min with a Haake PG 20 temperature programmer, connected with a Haake water circulating bath equipped with a refrigerator. The melting curves were obtained by monitoring the absorbance at 270 nm as a function of temperature. The concentration of DNA was determined by UV absorption in H_2O at 90°C, i.e. with DNA in the denaturated state, assuming as extinction coefficients 7500, 8500, 15000 and 12500 M^{-1} cm^{-1} for C, T, A and G, respectively (24).

Calorimetry

Differential scanning calorimetry (DSC) measurements were performed with a Setaram microcalorimeter. Scannings from 20 to 90°C and viceversa were done at the rate of 0.5°C/min. The DNA concentration employed was 5.2 mM/base; each cell contained about 0.9 ml of solution. Before scanning, the calorimeter was let overnight to reach thermal equilibrium and the calorimeter constant was checked by melting a standard solution of polyA:polyU which gave a ΔH value in good accord with the values reported in the literature.

Enzymatic Assay

The reaction of DNase I from bovine pancreas with DNA in both triple- and double-stranded forms was carried out in the acidic buffer. The DNase I was freshly prepared at a concentration of 1 mg/ml and it was used at different DNA/DNase I ratios: 11, 5.5, 3.6, 2.75, 1.0 at 30°C for 1.5 hours. The enzymatic reaction was blocked by adding to the reaction mixture β-mercaptoethanol (4% v/v). Then, the reaction products were heated at 60°C for 5′ and loaded into a denaturing (7 M urea) 20% acrylamide gel. The electrophoresis was carried out at room temperature for 3 hours at 25 V/cm.

Analysis of Transition Data

The experimental melting curves of the equimolar mixture between dR_{11} and dY_{24} were analyzed with a two-state model, as described below. The data were analyzed with a VAX computer, using the non-linear least-square algorithm of Marquardt (25). The program adjusted the parameters ΔH and ΔS of equation [4], minimizing the sum of squares of deviations between computed and experimental absorbance values. Moreover, the program provides the 95% confidence limits of the adjusted parameters.

RESULTS AND DISCUSSION

Design of H-DNA Structure

The pyrimidine strand dY_{24} is a 'mirror' repeated sequence, whose 3′-half can form a conventional antiparallel duplex with the purine strand dR_{11}, $(dR_{11}+).(dY_{24}-)$ [the signs + and − indicate the 5′→3′ and 3′→5′ strand directions, respectively]:

```
5′GAGAAGAAAGA                    (Scheme 1)
  . . . . . .
3′CTCTTCTTTCTTTTCTTTCTTCTC
```

If the dangling 5′-half of $d(Y_{24})$ folds back and binds to the major groove of the $(dR_{11}+).(dY_{24}-)$ duplex, a triple-stranded structure which mimicks H-DNA (9) is obtained. This triplex comprises two distinct domains: a non-bonded loop of four thymidines and a triple-stranded helix, stabilized by T:A:T and C:G:C^+ triads:

```
5′ C T C T T C T T T C
   + · + · · + · · · +
5′ G A G A A G A A A G   A   T4      (Scheme 2)
   . . . . . . . . . .
3′ C T C T T C T T T C
```

Since the formation of each C:G:C$^+$ triad requires the protonation of one cytosine, the triple-stranded structure is expected to be stabilized in moderately acidic conditions. In both types of triads the pyrimidines from the 5'-half of dY_{24} are hydrogen-bonded to the purines of dR_{11} through Hoogsteen pairings (10,19).

The loop built by the central bases of dY_{24} should comprise the four thymidines, in order to bridge the phosphate-phosphate distance between the C-C bases of the last C:G:C$^+$ triad: this distance is higher than that bridging a Watson-Crick helix. Thus, the T:A:T triad on the top of the stem can not form, in order to allow a four-member thymidine loop.

Electrophoresis

The tendency of dY_{24} and dR_{11} to form a triple helix was assayed by non-denaturating PAGE electrophoresis in standard buffer at pH=5. Figure 1a shows a 20% PAGE analysis of dY_{24} (lane g), dR_{11} (lane f) and $(dR_{11}).(dY_{24})$ mixture, at two different concentrations (lanes d and e). As a reference an 11-triad DNA triplex, recently characterized in our laboratories (1), was used (lane c). This reference triplex was obtained by mixing the hairpin form of d(GAAGGAGGAGATTTTTCTCCTCCTTC) with the strand d(CTTCCTCCTCT), in the same acidic buffer used in this work. Since the size (11 triads) and the base composition (48.6% C+G) of the reference DNA triplex are comparable to those of the triplex which should be formed by $(dR_{11}).(dY_{24})$ (10 triads, 34.3% C+G), both DNA structures should exhibit similar mobilities. Lanes d and e show that dY_{24} and dR_{11}, in equimolar mixture, co-migrate in the gel and exhibit a mobility analogous to that shown by the reference triplex. The weak bands of lower mobility are probably due to a minor presence of double length triplexes as $(dY_{24}-).(dR_{11}+)_2.(dR_{11}-)_2$ and/or $(dY_{24}+).(dR_{11}\pm)_2.(dY_{24}-)$, the former being favored by the presence of Mg^{2+} (26). The electrophoretic profiles of lanes d and e strongly suggest that also dY_{24} and dR_{11} can form a triple-stranded structure, at pH=5. This is corroborated by the fact that both the reference triplex and $(dR_{11}).(dY_{24})$ show similar hydrodynamic properties, as revealed by the Ferguson plots of the relative mobility versus acrylamide concentration (27) (Figure 1b), according to the equation

$$\log R_f = \log R_f(0) - K_R C$$

where R_f is the relative mobility of the DNA structures in the gel of composition C in acrylamide, while $R_f(0)$ represents the relative mobility for C→0. The slope K_R of the plot provides an estimate of the retardation coefficient of the DNA structures: a constant related to the size and shape of the DNA itself (27). Figure 2a shows that both the $(dR_{11}).(dY_{24})$ and the reference triplex are characterized by similar K_R values, which are different from the value of a 12-mer duplex.

Alternatively, the $(dR_{11}).(dY_{24})$ mixture could adopt a $(dR_{11}+).(dY_{24}-)$ duplex structure, with a dangling end (Scheme 1). However, the results obtained with fluorescence and enzymatic assays (see below) clearly indicate that the above duplex is not adopted by $(dR_{11}).(dY_{24})$ in the buffer at pH=5.

Fluorescence Assay

When ethidium intercalates between adjacent base-pairs of double-stranded DNA, its intrinsic fluorescence is considerably enhanced (28). By contrast, the fluorescence enhancement of

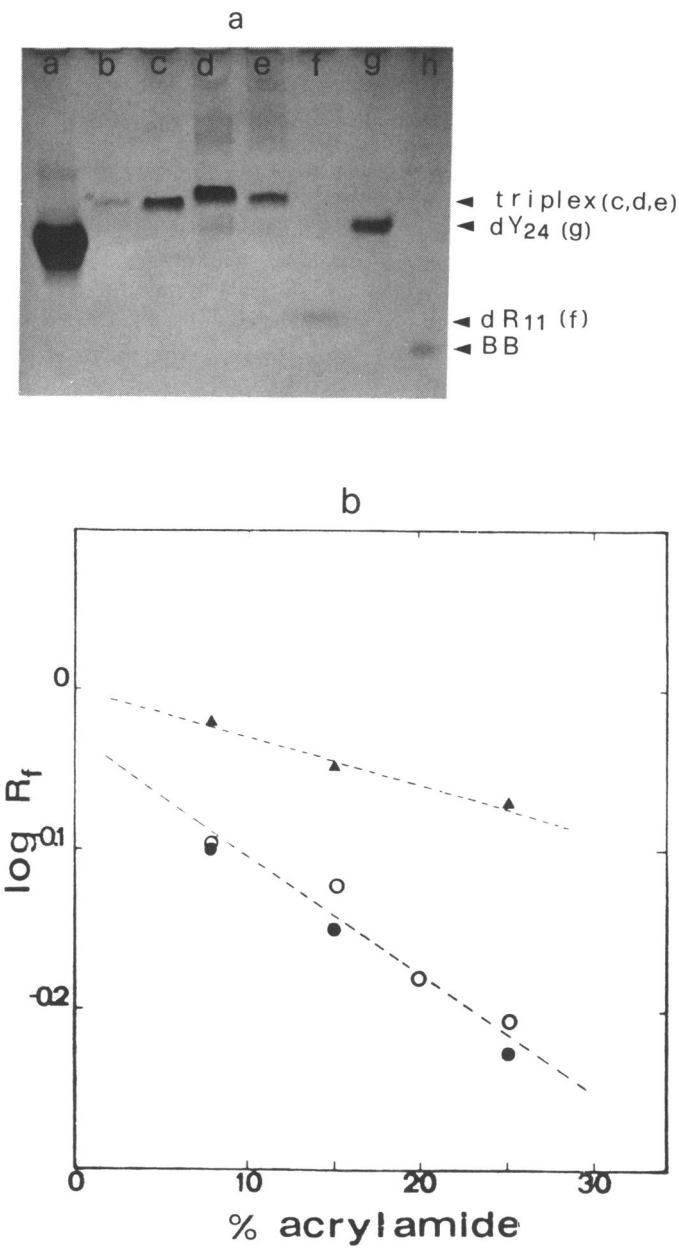

Figure 1. Panel A: 20% polyacrylamide gel electrophoresis of oligomers dY_{24}, dR_{11}, and equimolar mixture $(dY_{24}).(dR_{11})$. In each lane about 3 μg of DNA were loaded . Lanes a, b and c contain three reference sequences: a 14-mer, a 20-mer and an 11-triad DNA triplex, obtained by mixing the hairpin form of d(GAAGGAGGAGATTTTTCTCCTCCTTC) with d(CTTCCTCCTCT). Strands dY_{24} and dR_{11} were loaded in lanes g and f, respectively. Lanes d and e contain the $(dY_{24}).(dR_{11})$ mixture at concentrations one double to the other. The experiment was conducted in 0.1 M sodium acetate (pH=5), 10 mM $MgCl_2$, 10 mM NaCl and at a voltage of 6V/cm. Panel B: Ferguson plots of the relative mobilities (mobility respect to that of d(GAAGGAGGAGCTTTTTCTCCT-CCTTC hairpin) for a 12-mer duplex (▲), $(dR_{11}).(dY_{24})$ (●), and for the reference triplex (○).

ethidium in the presence of triple- and single-stranded DNA is negligible (29). Thus, ethidium was used as a probe to test the triple-stranded structure formation by the $(dR_{11}).(dY_{24})$ mixture. Figure 2 shows the enhancement of ethidium fluorescence in buffers at pH=8 and pH=5, as a function of increasing amounts of the $(dR_{11}).(dY_{24})$ mixture, previously stabilized in the acidic buffer. At pH=8, a marked enhancement of fluorescence was observed as $(dR_{11}).(dY_{24})$ was added to the dye solution. This

suggests that at neutral pH the triplex does not form or, at least, it is easily converted to a normal duplex by the presence of ethidium. It should be remembered that the pKa of the cytosine residue is 4.3 (1), therefore the C:G:C^+ triads can hardly form at pH=8. By contrast ethidium fluorescence is only slightly enhanced by the presence of (dR_{11}).(dY_{24}) at pH=5. This indicates that in this acidic buffer the mixture does adopt a structure different from a duplex, for which the dye shows a poor affinity. The moderate increase of fluorescence observed at pH=5 can be attributed to a slight shift to the right of the (dR_{11}).(dY_{24}) triplex ⟷ (dR_{11}+).(dY_{24}−) duplex equilibrium, caused by ethidium.

DNase I Assay

A further evidence that the equimolar mixture of dY_{24} and dR_{11} adopts at pH=5 a triple-stranded structure was obtained with a DNase I assay. The effect of the nuclease on (dR_{11}).(dY_{24}) and on a 12-mer duplex was investigated by analyzing the products of an enzymatic digestion with electrophoresis in denaturing conditions. Figure 3 shows a 20% PAGE of (dR_{11}).(dY_{24}) and a 12-mer duplex after they have been incubated with increasing amounts of DNase I for 1.5 hours, at 30°C, in the acidic buffer. Lanes a and f contain the (dR_{11}).(dY_{24}) mixture and a 12-mer duplex untreated with DNase I, whereas lanes b−e and g−l contain the same samples, respectively, but after having been digested with increasing amounts of DNaseI. The electrophoresis shows that, while the 12-mer duplex is quickly degraded by DNase I within 1.5 hours, the (dR_{11}).(dY_{24}) mixture is resistant to the enzyme, even at the highest enzyme/triplex ratio. When the experiment was conducted at enzyme/triplex ratios five times higher, the bands of the 12-mer duplex disappeared completely from the lanes, while those of dY_{24} and dR_{11} remained in the gel (data not shown). Thus, (dR_{11}).(dY_{24}) is not a substrate for DNase I, as already has been observed for the reference triplex (1) and other DNAs in triple helix (29).

As for the low intensity of the dR_{11} bands, we have checked that it is due to a lower staining efficiency of the dye for the oligopurinic strand with respect to the oligopyrimidinic one.

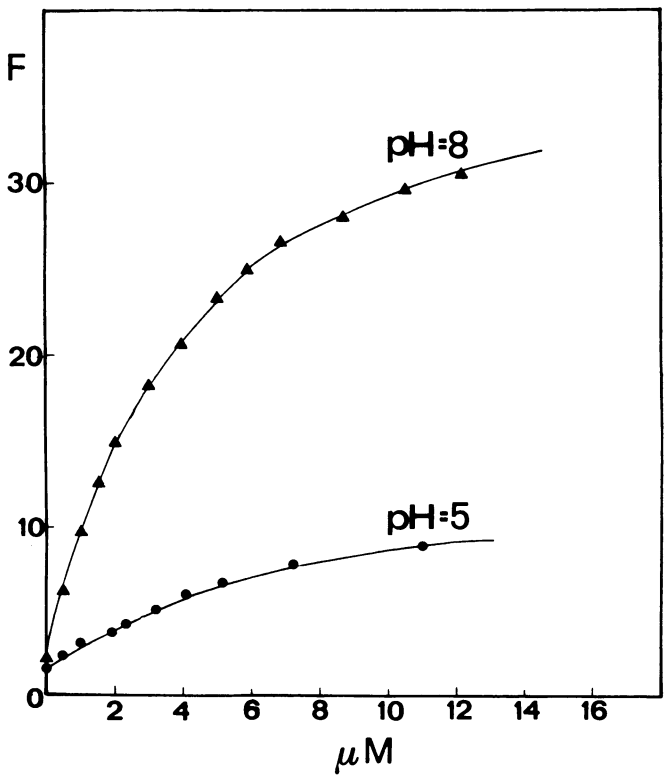

Figure 2. Increment of ethidium quantum yield as a function of increasing amounts of (dR_{11}).(dY_{24}) in buffers at pH=5 and pH=8. Initial dye concentration was 2.5 μM. The concentration of (dR_{11}).(dY_{24}) is expressed in μM of (dR_{11}).(dY_{24}) mixture.

Circular Dichroism

Figure 4 shows the circular dichroism spectrum of the (dR_{11}).(dY_{24}) mixture in the buffer at pH=5. The spectra of dR_{11} and dY_{24} are also reported. The mixture shows a spectrum very similar to that observed for the reference DNA triplex (1). In particular, both triplexes exhibit a large ellipticity at 280 nm, a crossover at 262 nm, and two negative bands at 245 and 212 nm, respectively. The CD spectrum of (dR_{11}).(dY_{24}) at pH=8 does not show the negative band at 212 nm (data not shown). This band, which characterizes also the CD spectra of polynucleotides in triple helix (29), could be considered as diagnostic of DNA triple-stranded formation.

Thermodynamics of Triplex Formation

UV-Melting

Figure 5 shows typical UV-absorbance (270 nm) versus temperature profiles for the (dR_{11}).(dY_{24}) mixture in buffers at pH=5 and at pH=8. The different melting behaviour observed offers another evidence that (dR_{11}).(dY_{24}) adopts diverse conformations in the two media.

We have seen that in the buffer at pH=5, the (dR_{11}).(dY_{24}) mixture forms a DNA triplex, therefore it can be assumed that the melting profiles obtained in this buffer is due to the triplex-to-coil transition. The triplex melts with a cooperative transition, characterized by an hyperchromicity of 24%. On renaturation the transition is almost exactly reproduced (Figure 5), indicating that the process of triple helix formation is quickly reversible. This behaviour is consistent with that observed for the reference DNA triplex (1), and with the finding that the interconversion between duplex and triplex structures, formed by (dR_n).(dY_n)

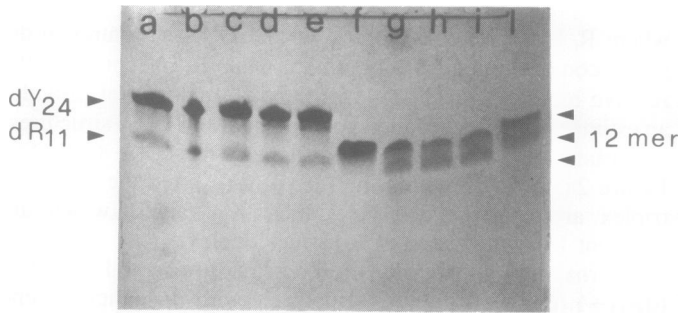

Figure 3. Denaturing gel electrophoresis of equimolar mixture (dR_{11}).(dY_{24}) and d(CGTCGCGCGACG) after 1.5 hours incubation at 30°C with increasing amounts of DNase I. The incubation buffer was 0.1 M sodium acetate (pH=5), 50 mM NaCl, 10 $MgCl_2$. Lanes a and g contain the (dR_{11}).(dY_{24}) and d(CGTCGCGCGACG), respectively, untreated. Lanes b-e and g-l contain (dR_{11}).(dY_{24}) and d(CGTCGCGCGACG) digested with DNase I at the following μgDNA/μgDNaseI ratios: 5.5, 1.0, 3.6, 2.75. The gel was obtained in 0.1 M sodium acetate (pH=5), 10 mM $MgCl_2$, 10 mM NaCl, 7 M urea buffer.

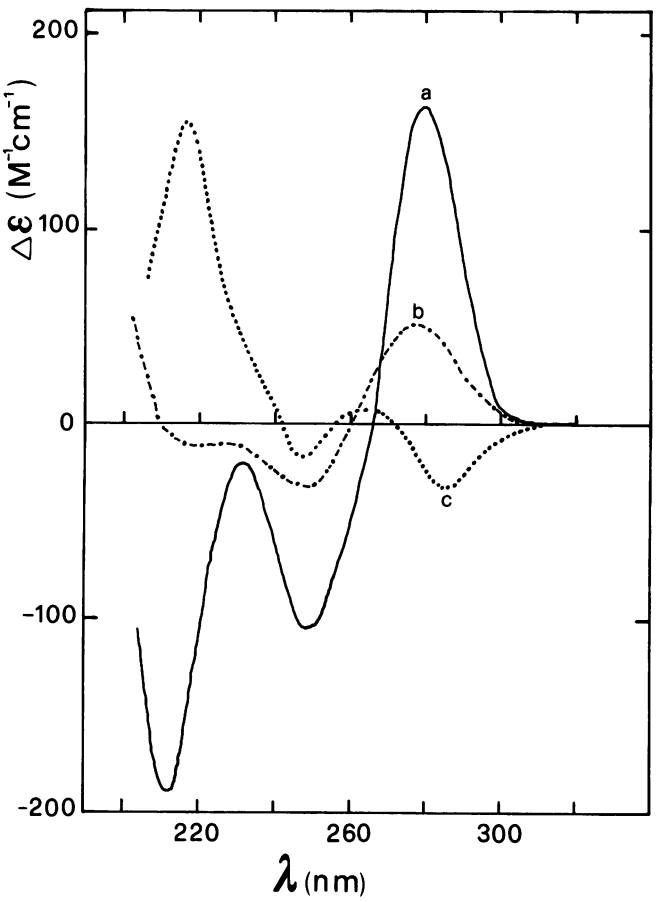

Figure 4. Circular dichroism spectra for dY_{24} (b), dR_{11} (c) and $(dR_{24}).(dR_{11})$ mixture (a) in 0.1 M sodium acetate (pH=5), 10 mM $MgCl_2$, 10 mM NaCl, at room temperature. The nucleotide concentration of $(dR_{24}).(dR_{11})$ is 4 mM.

sequences inserted in plasmids, is fast (30). We have performed a number of melting experiments at different nucleotide concentrations and the results are reported in Table I. The observation that the T_m of the transition changes with the DNA concentration suggests that the melting process is bimolecular, as one would expect for a one-step disruption of the $(dY_{24}).(dR_{11})$ triplex. By contrast, at pH=8, the $(dR_{11}).(dY_{24})$

Table I. Thermodynamic parameters for the triplex-coil transition of $(dR_{11}).(dY_{24})$ in sodium acetate 0.1 M (pH=5), 50 mM NaCl, 10 mM $MgCl_2$.

From UV-melting curves			
C_T (M/strand)	T_m[(a)] (°C)	$\Delta H^T_{VH}(UV)$[(b)] (kcal/mol)	$\Delta S^T_{VH}(UV)$[(b)] (e.u.)
2.1×10^{-6}	53.1	123 (±8)	348 (±24)
2.6×10^{-6}	53.6	129 (±9)	367 (±28)
8.3×10^{-6}	54.9	138 (±12)	394 (±38)
6.0×10^{-5}	56.8	136 (±7)	391 (±23)
2.9×10^{-4}	60.9[(c)]	–	–
– Average ΔH^T		131 (±12)	
$-\Delta H^T$ from $1/T_m$ vs ln C_T		143 ± 14 kcal/mol	

From DSC calorimetry		
Scanning	ΔH^T(cal)[(e)] (kcal/mol)	ΔH^T_{VH}(cal)[(f)] (kcal/mol)
1 Denaturation[(d)]	126	147
2 Rinaturation[(d)]	133	139
3 Rinaturation[(d)]	129	134
– Average ΔH^T	129 (±6)	140 (±14)

(a) T_m values are obtained form eq. [2] when $\alpha=0.5$. Experimental T_m values have an uncertainty of ±1°C; (b) the number in parenthesis represents the magnitude of the 95% confidence limits of ΔH and ΔS, as computed by the Marquardt algorithm (25); (c) data from DSC experiments; (d) DNA concentration is 5.2 mM/base; (e) ΔH^T(cal) is the calorimetric enthalpy change calculated from the area under the DSC curve; (f) ΔH^T_{VH}(cal) is the van 't Hoff enthalpy change calculated from the integrated heat capacity curve, according to equation [6].

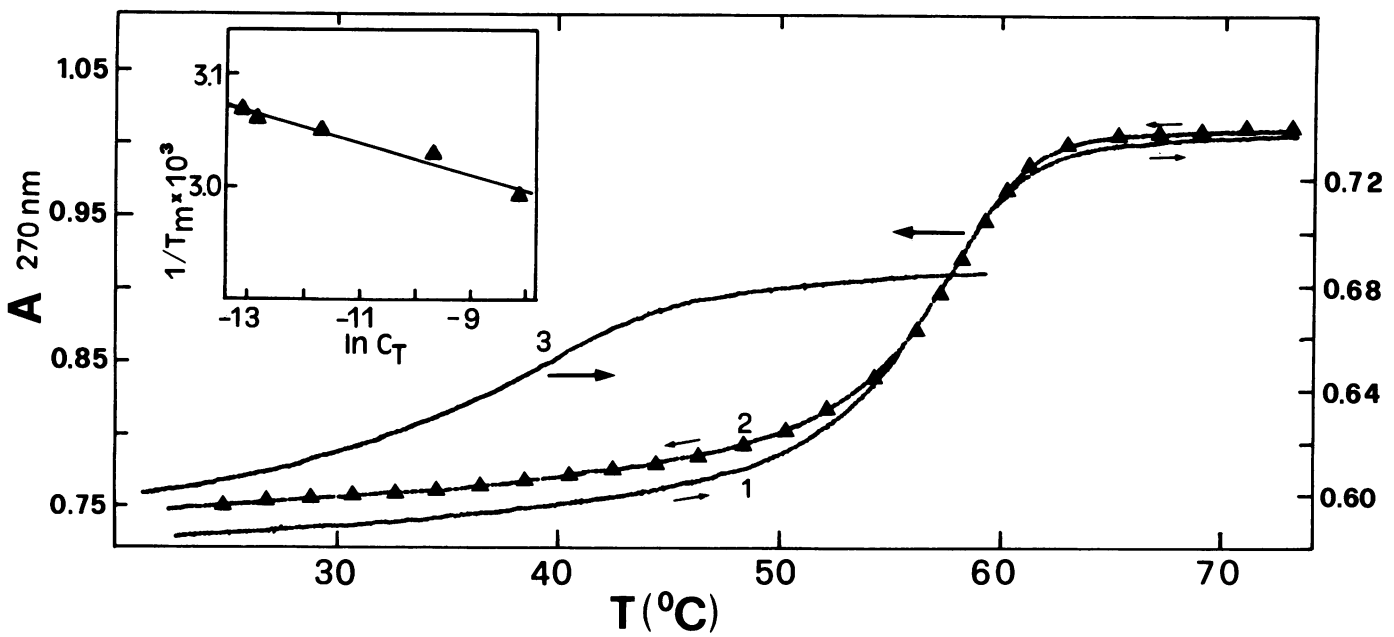

Figure 5. Absorbance (270 nm) versus temperature profiles for the $(dR_{11}).(dY_{24})$ mixture in 0.1 M sodium acetate (pH=5), 10 mM $MgCl_2$, 10 mM NaCl (curve 1: denaturation, curve 2: renaturation) and in the buffer at pH=8 (curve 3). The sample concentration was 60.5 μM/strand for curves 1 and 2, and 88 μM/strand for curve 3. The points (▲) on curve 2 are from the best-fit of this renaturation curve to eq. [4], using $\Delta H^T=136$ kcal/mol, $\Delta S^T=391$ e.u. Insert show the plot of reciprocal T_m versus ln C_T.

mixture melts at lower temperature (T_m=39°C), with a less cooperative transition, characterized by an hyperchromicity of 15 % only. This behaviour should reflect the denaturation of the (dR_{11}+).(dY_{24}−) duplex (Scheme 1). The enthalpy change associated with the duplex ⇌ coil transition of (dR_{11}+).(dY_{24}−), calculated with equations [2] and [4] (see below), by assuming a two-state model (31), is 74 kcal/mol. This ΔH value is nicely in agreement with that expected for the denaturation of the (dR_{11}+).(dY_{24}−) duplex (ΔH=78 kcal/mol), according to nearest-neighbor energy values (32,33).

Considering that the (dR_{11}).(dY_{24}) triplex is formed by short oligodeoxynucleotides and that the melting process is reversible and monophasic, we describe the triplex-to-coil transition by a two-state model:

$$\text{Triplex} \overset{K_T}{\rightleftharpoons} dR_{11} + dY_{24} \qquad [1]$$

whose equilibrium constant K_T is given by:

$$K_T = \alpha^2 C_T/(1-\alpha) = \exp(\Delta H^T/RT + \Delta S^T/R) \qquad [2]$$

where α is the fraction of DNA in single-stranded (coil) form at temperature T, C_T is the concentration of the dY_{24} strand, which is equal to that of dR_{11}, and H^T and S^T are the overall enthalpy and entropy changes of triple helix disruption.

The optical density of the solution containing the (dY_{24}).(dR_{11}) triplex is given by:

$$OD(T) = (\epsilon_T (1-\alpha) + \epsilon_C \alpha)C_T \qquad [3]$$

where ϵ_T, $\epsilon_C=(\epsilon_{dY}+\epsilon_{dR})/2$ are the extinction coefficients for the DNA in the triplex- and single-stranded forms, respectively. Combining equations [2] and [3] we obtain:

$$OD(T)= \{\epsilon_T + (\epsilon_C-\epsilon_T)\,[K_T/(2C_T)]\,[(1+4C_T/K_T)^{1/2}-1]\}C_T \qquad [4]$$

Equation [4] was fitted to the experimental melting curves with a non-linear least-square program (algorithm of Marquardt (25)), leaving as adjustable parameters ΔH^T and ΔS^T. The extinction coefficients ϵ_T and ϵ_C were assumed to be linear functions of the temperature with slopes that were determined from the extended pre- and post-transition regions of the experimental melting curves. Table I collects the results of a number of best-fit analyses performed on melting curves of the (dR_{11}).(dY_{24}) mixture at different DNA concentrations. The theoretical curves computed using equation [4] describe with accuracy the experimental ones (Figure 5): the difference between experimental and calculated OD values was in general within 1%. For each best-fit we have also reported the 95% confidence limits on ΔH and ΔS. Table I shows that the uncertainty on ΔH and ΔS is about 10%, a magnitude typical for this type of analysis (34).

Another way to calculate the ΔH^T for the triplex-to-coil transition was obtained by plotting the reciprocal semitransition values, T_m, versus $\ln C_T$ according to (35,36):

$$1/T_m = R\ln C_T/\Delta H^T + \Delta S^T/\Delta H^T \qquad [5]$$

From the slope of this plot (insert of Figure 5) we obtained a value of $\Delta H^T = 143 \pm 14$ kcal/mol, in reasonable accord with that obtained by best-fit analyses of the melting profiles.

Differential Scanning Calorimetry

Figure 6a shows the excess heat capacity versus temperature curve obtained by DSC microcalorimetry for (dY_{24}).(dR_{11}) in the buffer at pH=5. The buffer baseline is also reported. The calorimetric ΔH^T(cal) was determined by the area under the excess heat capacity curve. Figure 6b shows the integrated (and normalized) differential DSC curve. This integral curve was used to estimate the van 't Hoff enthalpy change from calorimetric data according to the relation (36):

$$\Delta H^T_{VH}(cal) = 6RT_m^2(d\alpha/dT)_{Tm} \qquad [6]$$

where $T=T_m$ when $\alpha=0.5$. Values of ΔH^T(cal) and ΔH^T_{VH}(cal) from three DSC experiments are reported in Table II. The calorimetric enthalpy value for the triplex-coil transition of (dY_{24}).(dR_{11}) is $\Delta H^T(cal) = 129 \pm 6$ kcal/mol, whereas the $\Delta H^T_{VH}(cal)$ is 140 ± 14 kcal/mol.

An insight into the nature of the transition was obtained by comparing the calorimetric and the van 't Hoff values of ΔH^T. While the van 't Hoff ΔH^T depends on the model assumed to describe the transition, the calorimetric ΔH^T is model-independent, this quantity being directly obtained by the area under the DSC peak. Thus, the ratio $\Delta H^T_{VH}/\Delta H^T(cal) \approx 1$ suggests that the triplex-coil transition of (dR_{11}).(dY_{24}) proceeds, with a good approximation, in a two-state manner (31).

The contribution to ΔH^T due to the 10 base pair Watson-Crick helix (Scheme 1) is estimated to be 67 kcal/mol: 74 kcal/mol (exptl. value at pH=8) minus 7 kcal/mol due to one TC/AG stacking (32,33), which is lost on triplex formation. Thus, we found that the triplex-duplex transition is characterized by a ΔH of 62 kcal/mol. Considering that the triplex is made by 10 triads, it follows that each pyrimidine residue accomodating in the major groove of the duplex is accompanied by about 6.2 ± 0.6 kcal/mol. This value comprises also the contribution from the cytosine protonation for the formation of the four C:G:C^+ triads, and the possible contribution due to the B→A transition of the Watson-Crick helix, which, however, should be quite small.

We have previously seen for the reference DNA triplex, whose C+G contents is 48.6%, that the contribution to ΔH^T from C protonation is about 10% (1). Since in (dR_{11}).(dY_{24}) the C+G contents is 34.3%, the C protonation will contribute to ΔH^T for less than 10%. Thus, the enthalpy change for each pyrimidine binding into the major groove with a Hoogsteen pairing, less the protonation contribution, should be at least 5.8 ± 0.6 kcal/mol. This value is in reasonable accord with that of 6.6 ± 0.7 kcal/mol found for the reference triplex. The possible slight difference could be attributed to a different content of C:G:C^+ triads in the two triplexes. To this regard it should be noted that the thermostability of DNA triplexes, obtained from (dR_n).(dY_n) sequences inserted in plasmids, increases with the G+C content: a triplex with 67% G+C was 12°C more stable than one with 25% G+C (30). Our results could suggest that the increased stability of C+G rich triplexes is enthalpic in origin.

Effect of Triad Interruptions on the Stability of Triplex

The effect on the stability of DNA triplexes due to interruptions in the (dR_n).(dY_n) sequence has been reported (30). A single interruption was obtained by inverting two complementary nucleotides of the (dR_n).(dY_n) sequence, so that one pyrimidine was introduced into the purine strand (30). This resulted in A:T:A and A:T:T triads, which were found to destabilize a 12-triad DNA triplex by 5 and 7°C, respectively.

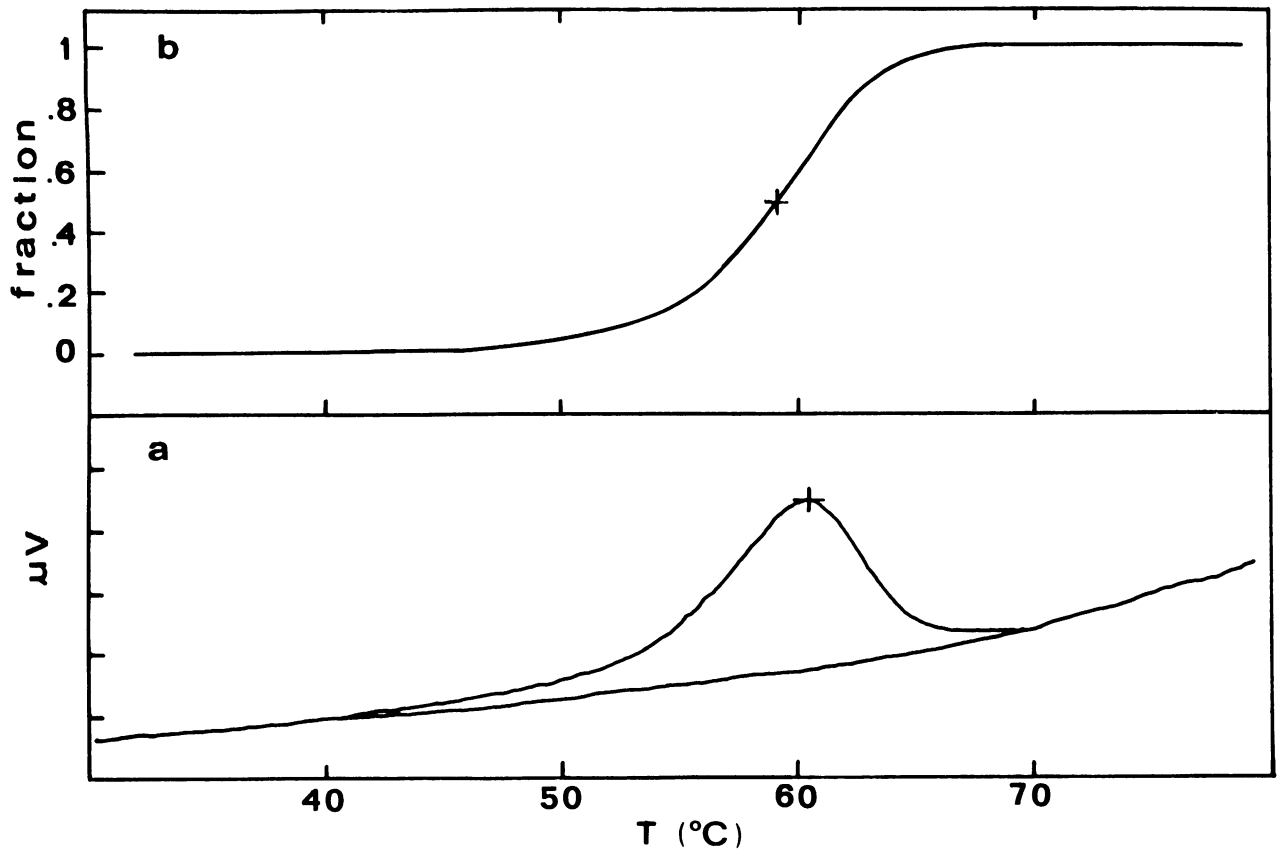

Figure 6. Panel A: Excess heat capacity curve for the renaturation of the $(dR_{11}).(dY_{24})$ in 0.1 M sodium acetate (pH=5), 10 mM $MgCl_2$, 10 mM NaCl, at the DNA concentration of 5.2 mM/base. Scanning has been performed from 90 to 20°C, at the temperature rate of 0.5°C/min. Panel B: Normalized curve obtained by integration of the differential heat capacity curve.

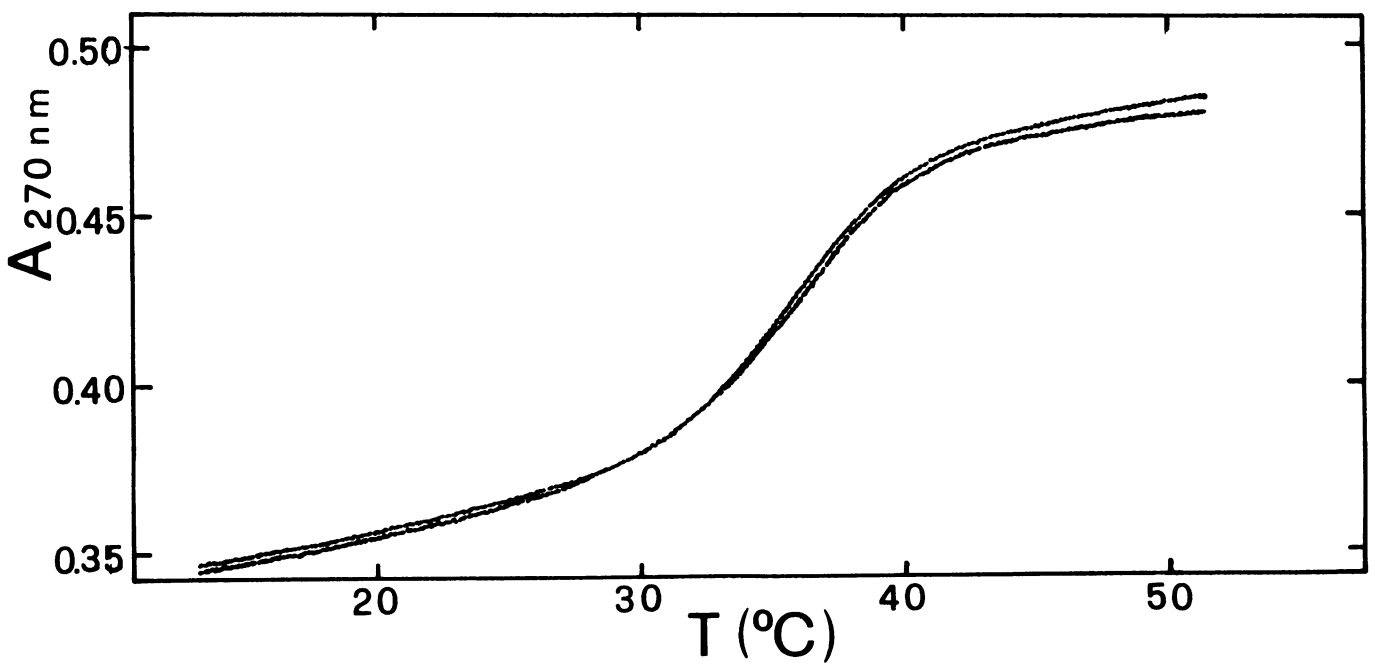

Figure 7. Absorbance (270 nm) versus temperature profiles for the equimolar mixture between dY_{24} and d(GAGTAGAAAGA), forming a triplex with a T:T:T triad. The curves, in denaturation and renaturation, have been obtained in 0.1 M sodium acetate (pH=5), 50 mM $MgCl_2$, 10 mM NaCl. Strand concentration is 6.6 μM.

Oligomer d(GAGTAGAAAGA) differs from (dR_{11}) for having one A replaced by one T. When this oligomer is complexed with dY_{24}, a 10-triad DNA triplex with one T:T:T is formed. This triplex is found to be less stable with respect to that of (dR_{11}).(dY_{24}) by 18°C, in the same solvent (Figure 7). The denaturation profile for this imperfect triplex is found to be reversible and significantly broader compared to the profile exhibited by (dR_{11}).(dY_{24}). The enthalpy change of the transition, calculated on the basis of a two-state model, is $\Delta H^T_{VH} = 103 \pm 10$ kcal/mol, considerably lower than that obtained for the perfect (dY_{24}).(dR_{11}) triplex. To establish whether this lower ΔH^T is due to a real enthalpic destabilization of the triplex or to the untenability of a two-state model to describe this transition, cannot yet be decided. In any case the result shows that the presence of one T:T:T triad, although tolerated by the 10-triad triplex, determines a marked reduction in its thermostability.

ACKNOWLEDGMENT

This work has been carried out with the financial support of Italian Ministry of Education, and Italian National Research Council (contribution n. 88.03479.04).

REFERENCES

1. Manzini, G., Xodo, L.E., Gasparotto, D., Quadrifoglio, F., van der Marel, G.A. & van Boom, J, H.(1990) J.Mol.Biol. **213**, (in press).
2. Riley, M., Maling, B., Chamberlin, M.J.(1966) J.Mol.Biol.**20**, 359–389.
3. Michelson, A.M., Massoulié, J., Guschlbauer, W.(1967) Prog. Nucleic Acids Mol.Biol. **6**, 83–141.
4. Morgan, A.R., Wells, R.D.(1968) J.Mol.Biol. **37**, 63–80.
5. Sarocchi, M.-T., Courtois, Y., Guschlbauer, W.(1970) Eur.J.Biochem. **14**, 411–421.
6. Marck, C., Thiele, D.(1978) Nucl. Acids Res. 5, 1017–1028.
7. Douglas, J.S., Johnson, D.A., Morgan, A.R. (1979) Nucl.Acids Res. **6**, 3073–3091.
8. Lee, J.S., Woodsworth, M.L., Latimer, L.J.P., Morgan, A.R. (1984) Nucl.Acids Res. **12**, 6603–6614.
9. Lyamichev, V.I., Mirkin, S.M., Frank-Kamenetskii, M.D. (1986) J.Biomol.Struct.Dyn.**3**, 667–669.
10. Mirkin, S., Lyamichev, V.I., Drushlyak, N.K., Dobrynin, V.N., Filippov, S.A., Frank-Kamenetskii, M.D. (1987) Nature (London) **330**, 495–497.
11. Wells, R.D., Collier, D.A., Hanvey, J.C., Shimizu, M., Wohlrab, F. (1988) FASEB J. **2**, 2939–2949.
12. Moser, H.E. & Dervan, P.B.(1987)Science **238**, 645–650.
13. Htun, H., Dahlberg, J.E. (1988) Science **241**, 1791–1795.
14. Behe, M.J.(1987) Biochemistry **26**, 7870–7875.
15. Birnboim, H.C., Sederoff, R.R., Peterson, M.C.(1979) Eur.J. Biochem. **98**, 301–307.
16. Larsen,A., Weintraub, H.(1982) Cell **29**, 609–622.
17. Htun, H., Lund, E., Dahlberg, J.E. (1984) Proc.Natl.Acad.Sci.USA, **81**, 7288–7292.
18. Pulleyblank, D.E., Haniford, D.B., Morgan, A.R. (1985) Cell **42**, 271–280.
19. Arnott,S., Selsing, E.(1974) J.Mol. Biol. **88**, 509–521.
20. François, J-C., Saison-Behmaaras, T., Hélène,C.(1988) Nucl. Acids Res. **16**, 11431–11440.
21. Rajagopal, P.& Feigon, J.(1989) Nature (London) 339, 637–640.
22. De Los Santos, C., Rosen, M. & Patel, D.(1989) Biochemistry **28**, 7282–7289.
23. Frank, R. & Koster, H.(1979) Nucl. Acids Res. **6**, 2069–2087.
24. Cantor, C.R. & Schimmel, P.R.(1980) Biophysical Chemistry, Part III, W.H.Freeman and Co., San Francisco.
25. Bevington, P.R.(1969) Data Reduction and Error Analysis for the Physical Sciences, Mc Graw-Hill, New-York.
26. Kohwi, Y. & Kohwi-Shigematsu, T. (1988) Proc.Natl.Acad.USA **85**, 3781–3785.
27. Roadbard, D. & Chrambach, A.(1971) Anal.Biochemm. **40**, 94–134.
28. LePecq, J.B.& Paoletti, C.(1967) J.Mol.Biol. **27**, 87–106.
29. Lee, J.S., Johnson, D.A.& Morgan, A.R.(1979) Nucl. Acids Res. **6**, 3073–3091.
30. Hanvey, J.C., Shimizu, M. & Wells, R.D. (1989) J.Biol.Chem. **264**, 5950–5956.
31. DePrisco-Albergo, D., Marky, L.A., Breslauer, K.J. & Turner,D.H. (1981) Biochemistry **20**, 1409–1413.
32. Breslauer, K.J., Frank, R., Blocker, H. & Marky, L.A.(1986) Proc. Natl. Acad. USA **83**, 3746–3750.
33. Gotoh, O. & Tagashira, Y. (1981) Biopolymers **20**, 1033–1042.
34. Freier, S.M., Alkema, D., Sinclair, A., Neilson, T., Turner, D.H. (1985) Biochemistry **24**, 4533–4539.
35. Martin, F.H., Uhlenbeck, O.C. & Doty, P. (1971) J.Mol.Biol. **57**, 201–215.
36. Marky, L.A. & Breslauer, K.J.(1987) Biopolymers **26**, 1601–1620.